What are Marine Ecological Time Series telling us about the ocean? A status report

[Individual Chapter (PDF) download]

The full report (all chapters and Annex) is available online at:

http://igmets.net/report

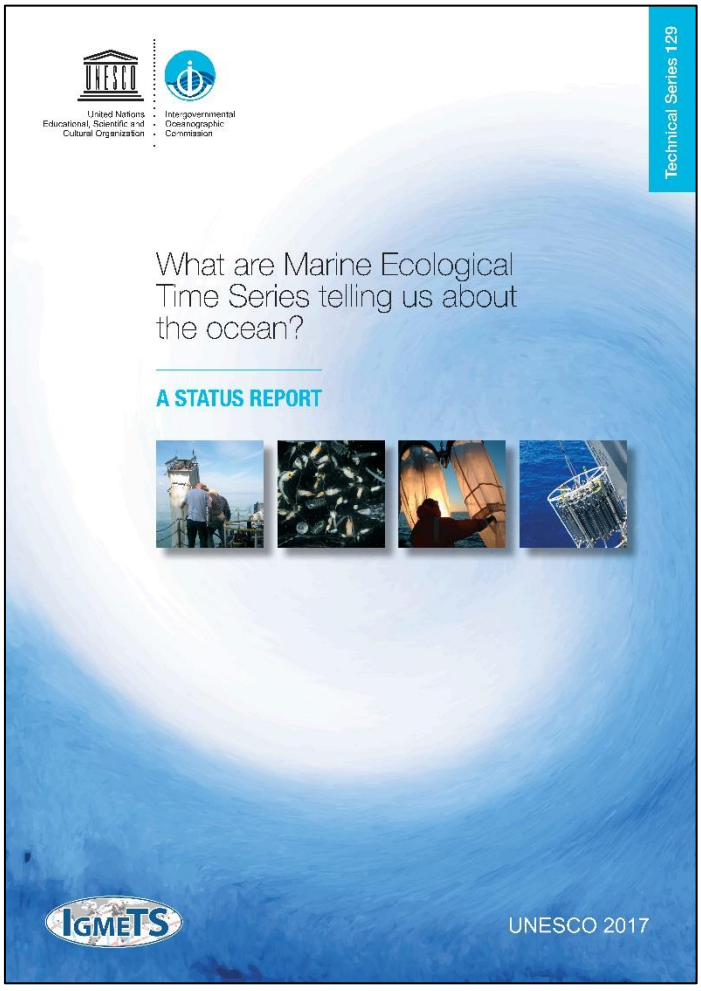

This page intentionally left blank

to preserve pagination in double-sided (booklet) printing

4 North Atlantic Ocean

Antonio Bode, Hermann W. Bange, Maarten Boersma, Eileen Bresnan, Kathryn Cook, Anne Goffart, Kirsten Isensee, Michael W. Lomas, Patricija Mozetic, Frank E. Muller-Karger, Laura Lorenzoni, Todd D. O'Brien, Stéphane Plourde, and Luis Valdés

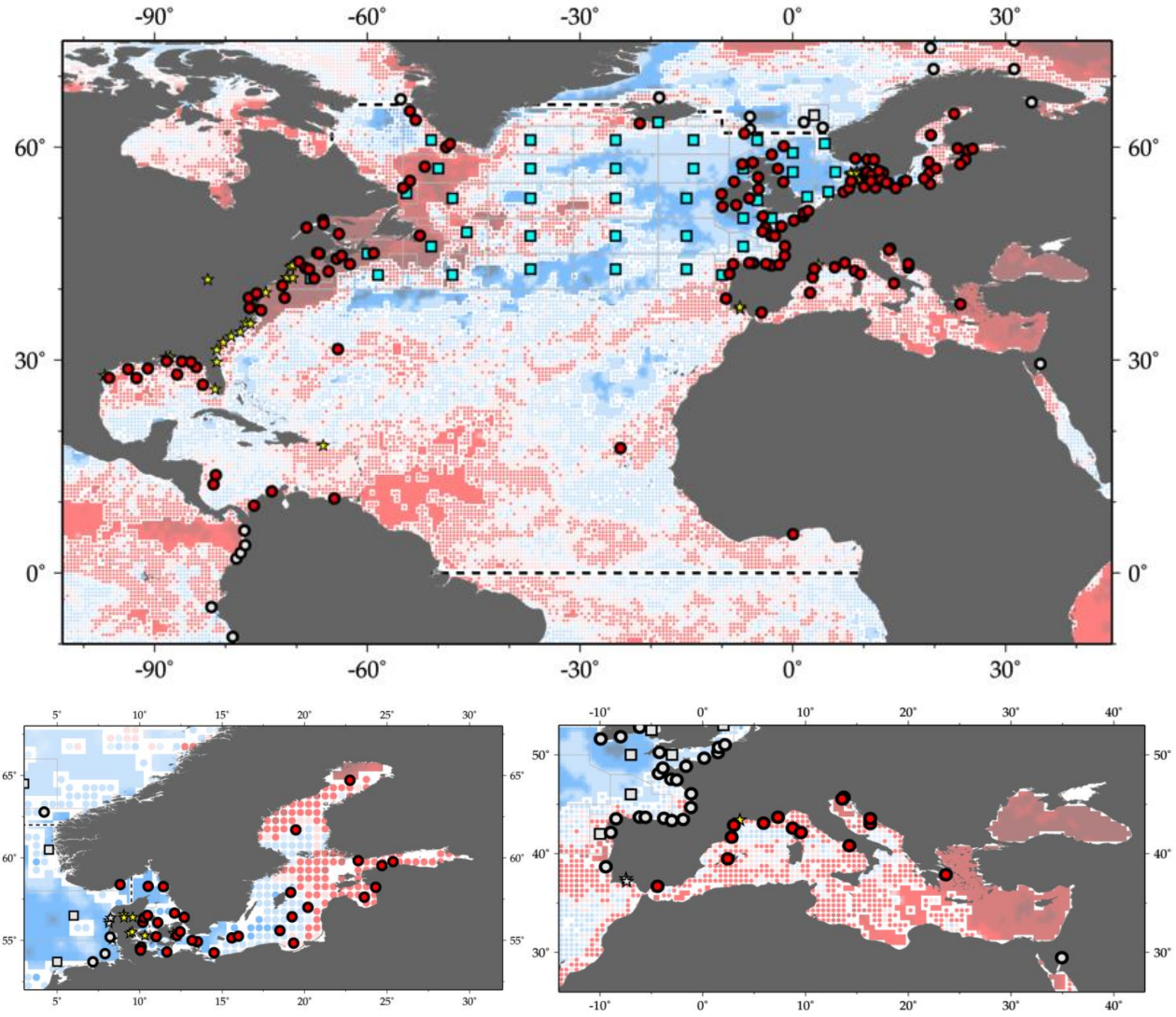

Figure 4.1. Map of IGMETS-participating North Atlantic time series, with zoomed insets for the Baltic Sea and Mediterranean Sea, on a background of a 10-year time-window (2003–2012) sea surface temperature trends (see also Figures 4.3, 4.8, and 4.9). At the time of this report, the North Atlantic collection consisted of 211 time series (coloured symbols of any type), of which 39 were from Continuous Plankton Recorder subareas (blue boxes), and 37 were from estuarine areas (yellow stars). Dashed lines indicate boundaries between IGMETS regions. Uncoloured (gray) symbols indicate time series being addressed in a different regional chapter (e.g. Arctic Ocean, South Pacific). See Tables 4.3–4.5 for a listing of this region's participating sites. Additional information on the sites in this study is presented in the Annex.

Participating time-series investigators

Eric Abadie, Jose L. Acuna, M. Teresa Alvarez-Ossorio, Anetta Ameryk, Jeff Anning, Elvire Antajan, Georgia Asimakopoulou, Yrene Astor, Angus Atkinson, Hermann Bange, Ana Barbosa, Nick Bates, Beatrice Bec, Radhouan Ben-Hamadou, Claudia Benitez-Nelson, Antonio Bode, Maarten Boersma, Angel Borja, Eileen Bresnan, Juan Bueno, Craig Carlson, Jacob Carstensen, Gerardo Casas, Claudia Castellani, Jacky Chauvin, Luis Chicharo, Epaminondas Christou, Nathalie Cochennec-Laureau, Amandine Collignon, Yves Collos, Kathryn Cook, Dolores Cortes, Joana Cruz, Maurizio Ribera D'Alcalà, Alejandro de la Sota, Alessandra de Olazabal, Laure Devine, Emmanuel Devred, Iole Di Capua, Rita Domingues, Anne Doner, Antonina dos Santos, Joerg Dutz, Martin Edwards, Joao Pedro Encarnacao, Luisa Espinosa, Tone Falkenhaug, Ana Faria, Maria Luz Fernandez de Puelles, Susana Ferreira, Bjorn Fiedler, James Fishwick, Serena Fonda-Umani, Almudena Fontan, Janja France, Javier Franco, Eilif Gaard, Peter Galbraith, Helena Galvao, Pep Gasol, Astthor Gislason, Anne Goffart, Renata Goncalves, Rafael Gonzalez-Quiros, Gabriel Gorsky, Annika Grage, Hafsteinn Gudfinnsson, Kristinn Gudmundsson, David Hanisko, Jon Hare, Roger Harris, Erica Head, Jean-Henri Hecq, Anda Ikauniece, Arantza Iriarte, Solva Jacobsen, Marie Johansen, Catherine Johnson, Jacqueline Johnson, Kevin Kennington, Georgs Kornilovs, Arne Kortzinger, Alexandra Kraberg, Nada Krstulovic, Aitor Laza-Martinez, Alain Lefebvre, Sirpa Lehtinen, Maiju Lehtiniemi, William Li, Priscilla Licandro, Michael Lomas, Christophe Loots, Angel Lopez-Urrutia, Laura Lorenzoni, Francesca Margiotta, Piotr Margonski, Jennifer Martin, Daniele Maurer, Maria Grazia Mazzocchi, Jesus M. Mercado, Claire Méteigner, Ana Miranda, Pedro Morais, Patricija Mozetic, Teja Muha, Frank Muller-Karger, Florence Nedelec, Vanessa Neves, Lena Omli, Emma Orive, Hans Paerl, Kevin Pauley, S.A. Pedersen, Ben Peierls, Pierre Pepin, Myriam Perriere Rumebe, Tim Perry, David Pilo, Sophie Pitois, Stephane Plourde, Arno Pollumae, Dwayne Porter, Lutz Postel, Nicole Poulton, A. Miguel P. Santos, Andy Rees, Michael Reetz, Beatriz Reguera, Jasmin Renz, Mickael Retho, Marta Revilla, M. Carmen Rodriguez, Gunta Rubene, Tatiana Rynearson, Rafael Salas, Danijela Santic, Diana Sarno, Michael Scarratt, Renate Scharek, Mary Scranton, Sergio Seoane, Stefanija Sestanovic, Mike Sieracki, Joe Silke, Ioanna Siokou-Frangou, Milijan Sisko, Tim Smyth, Mladen Solic, Dominique Soudant, Jeff Spry, Michel Starr, Deborah Steinberg, Lars Stemmann, Rowena Stern, Solvita Strake, Patrik Stromberg, Glen Tarran, Gordon Taylor, Maria Alexandra Teodosio, Robert Thunell, Valentina Tirelli, Ibon Uriarte, Luis Valdés, Victoriano Valencia, Marta M. Varela, Olja Vidjak, Fernando Villate, Norbert Wasmund, George Wiafe, Claire Widdicombe, Karen H. Wiltshire, Malcolm Woodward, Lidia Yebra, Cordula Zenk, Soultana Zervoudaki, and Adriana Zingone

This chapter should be cited as: Bode, A., Bange, H. W., Boersma, M., Bresnan, E., Cook, K., Goffart, A., Isensee, K., *et al.* 2017. North Atlantic Ocean. *In* What are Marine Ecological Time Series telling us about the ocean? A status report, pp. 55–82. Ed. by T. D. O'Brien, L. Lorenzoni, K. Isensee, and L. Valdés. IOC-UNESCO, IOC Technical Series, No. 129. 297 pp.

4.1 Introduction

The North Atlantic Ocean represents 46 million km² of the global ocean. This region (Figure 4.1) is characterized by unique geomorphological features that greatly affect water circulation and oceanographic processes, showing an asymmetry in surface temperature fields and currents that have no homologues in other ocean basins (Worthington, 1986; Marshall *et al*., 2001). In the North Atlantic, surface circulation at mid-latitudes is dominated by the Gulf Stream (Figure 4.2). This current veers off the American continent around Cape Hatteras (34°N). A divergence of this current around 40°N creates the southeasterly flow of the Azores Current and the northeasterly flow of the North Atlantic Current, both contributing to the gyre circulation in the central basin. The whole current system greatly influences heat flow and transport of water in the entire North Atlantic basin. The protuberance of Brazil and the Guianas in South America produces an asymmetry in the westward flow of the trade winds, allowing the flow of equatorial surface waters into the North Atlantic and eventually into the Gulf Stream and northern waters. The influence of the tropical heat carried by these waters extends northward of 60°N off Iceland. Restrictions to the bottom circulation imposed by the Mid-Atlantic Ridge topography also induce an asymmetry in the circulation between the eastern and western subbasins, thus causing measurable differences in the corresponding marine ecosystems (Longhurst, 2007).

The North Atlantic is one of the main regions of origin of deep ocean water. The North Atlantic Deep Water (NADW) is composed of several water masses formed by the winter cooling of surface waters at high latitudes. It is subsequently modified by deep convection and also by overflow of dense water across the Greenland–Iceland–Scotland Ridge (Dickson and Brown, 1994). In the North Atlantic, there are also several semi-enclosed seas (marginal seas) with specific oceanographic conditions, including the Caribbean Sea and Gulf of Mexico, Mediterranean, Black Sea, North Sea, and Baltic Sea.

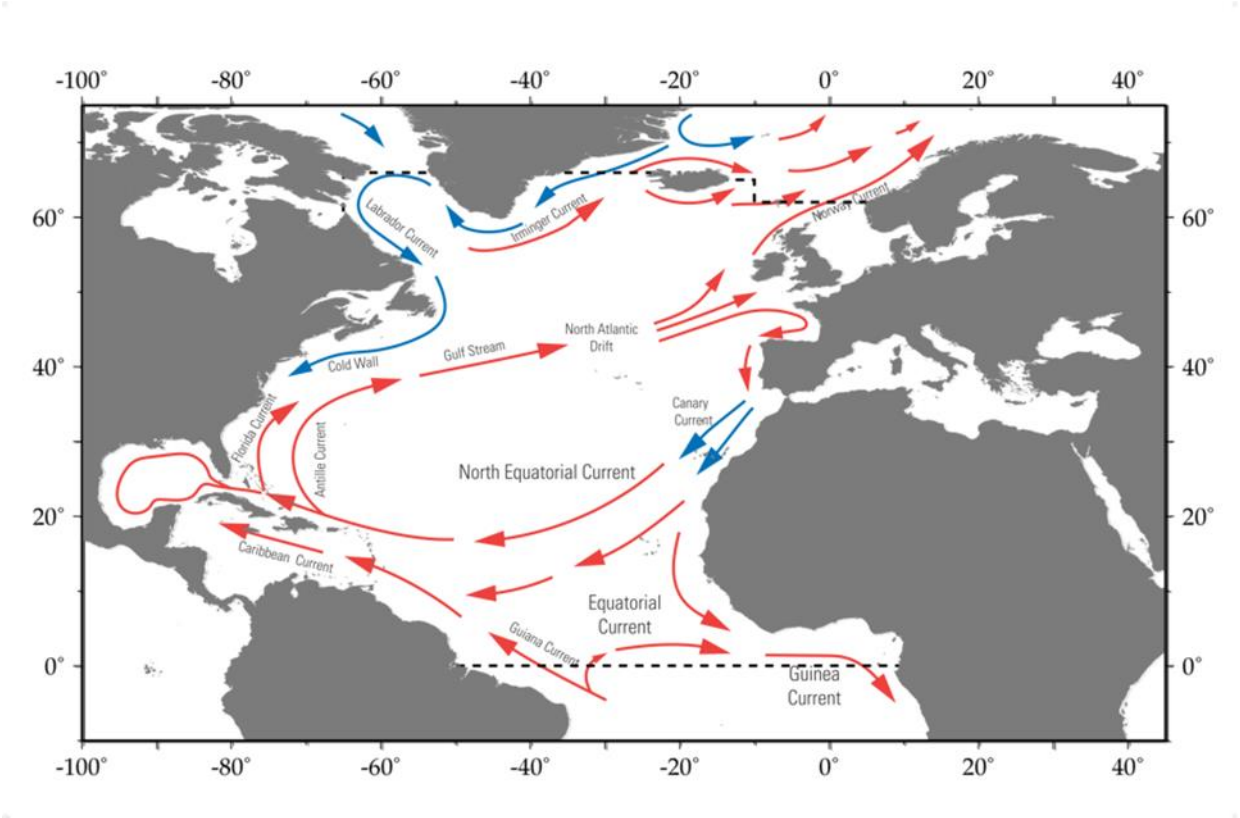

Figure 4.2. Schematic of major current systems in the IGMETS-defined North Atlantic region. Red arrows indicate generally warmer water currents; blue arrows indicate generally cooler water currents.

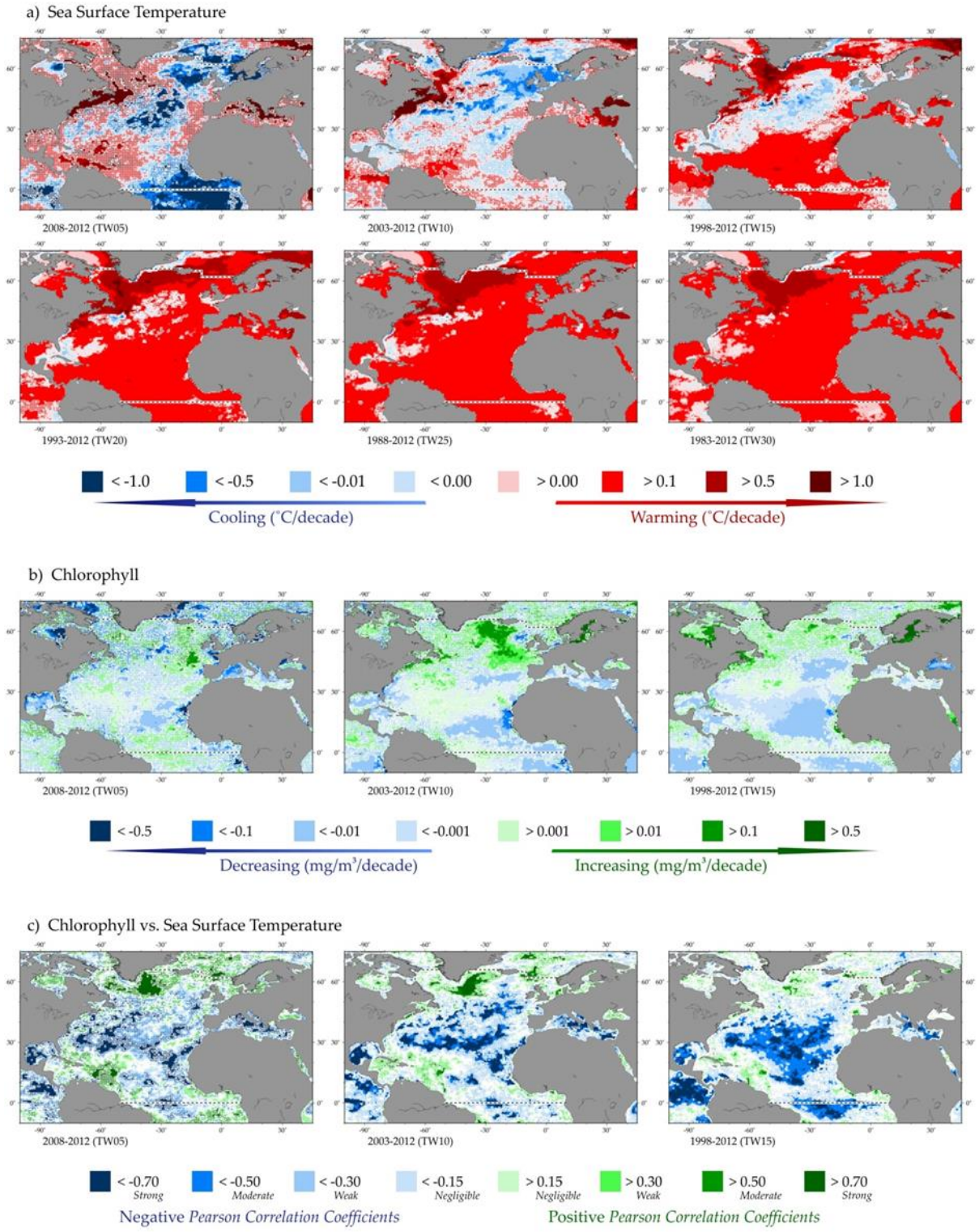

Figure 4.3. Annual trends in North Atlantic region (a) sea surface temperature (SST), (b) sea surface chlorophyll (CHL), and (c) correlations between CHL and SST for each of the standard IGMETS time-windows. See "Methods" chapter for a complete description and methodology behind this figure.

The general oceanography of the North Atlantic can be affected, but also affects the climatic index known as North Atlantic Oscillation (NAO), which is measured as variations in atmospheric pressure fields over the basin. The NAO influences the fluxes of heat and water, including precipitation, with important consequences for most ecosystem components (Hurrell and Dickson, 2004). However, there are additional climatic drivers modulating or even compensating the effects of the NAO at regional or local scale (Hemery *et al*., 2008). The North Atlantic shows periodic changes in surface temperature fields that are tracked as the Atlantic Multidecadal Oscillation (AMO, Knudsen *et al*., 2011), with measurable effects on ecosystems (Hernández-Fariñas *et al*., 2014).

In this chapter, we describe the main patterns derived from analysis of ecological time series compiled by IGMETS during 1983–2012 to illustrate some of the variability of marine ecosystems at multiannual and regional scales. More detailed tables and maps can be accessed in the interactive IGMETS Explorer:

http://igmets.net/explorer/

4.2 General patterns of temperature and phytoplankton biomass

Time series of gridded, large-scale observations derived from reanalysed *in situ* and satellite data (Reynolds OIv2-SST and OCCCI-Chl, see "Methods" chapter) indicated a general warming paralleled by a decrease in phytoplankton biomass. These trends were consistent across various time-windows (Table 4.1, Figure 4.3). Warming at a rate of 0.1–0.5°C decade^{-1} was significant for 86% of the region for the 30-year time-period (1983–2012), while during short time-periods, regional variability became increasingly important (Figure 4.3a). Indeed, some regions, such as the Mediterranean Sea, were almost completely affected by warming. Notwithstanding this general trend, local cooling was observed in the eastern and central Atlantic when considering recent years (10- and 5-year time-windows).

In contrast to the SST trends, changes in chlorophyll were more heterogeneous and, considering the 15-year time-window, the general decrease of up to 0.01 mg Chl *a* m^{-3} decade^{-1} observed was only significant for 38% of the region (Table 4.2). However, changes in enclosed seas affected over a larger area, as in the Mediterranean, or were completely divergent from the general trend, as occurred in the Baltic where surface chlorophyll increased >0.5 mg Chl *a* m^{-3} decade^{-1} in the 10- and 15-year time-windows (Figure 4.3b). In all cases, the spatial patchiness in the trends increased in the analysis of shorter time-windows, likely as a result of local drivers. For example, when comparing the 10- and 5-year time-windows for SST (Figure 4.3a), some regions showed reversed trends, such as the Caribbean (which cooled over the 10-year time-window, but warmed over the 5-year window). The same occurred with satellite-derived chlorophyll, particularly in the Northwest Atlantic where it decreased over the 5-year time-window, but showed an increasing trend for the 10-year period (Figure 4.3b). Nevertheless, over the past 15 years, there has been a consistent increase in surface chlorophyll over most of the continental margins and the open North Atlantic (north of 50°N), while there was a decrease in the central regions of the North Atlantic (Figure 4.3b).

Warming was negatively correlated with chlorophyll in most of the region (Figure 4.3c), including the subtropical gyre and marginal seas (Caribbean and Mediterranean), but there was a positive correlation between SST and chlorophyll in some regions, such as at East Greenland and the subpolar North Atlantic. At the longest time-window considered (15-year time-window), there was a distinct latitudinal difference in the correlations, with most of the area located south of 50°N showing negative correlations both variables. Not excluding direct effects of temperature on the physiological processes of phytoplankton, these relationships also support a key role of stratification as the driver of changes in phytoplankton production either by limiting the input of nutrients from deep layers in already stratified regions (Behrenfeld *et al*., 2015) or by enhancing the access of phytoplankton to light in already mixed waters (Tremblay and Gagnon, 2009).

Table 4.1. Relative spatial areas (% of the total region) and rates of change within the North Atlantic region (including the Baltic Sea and Mediterranean Sea) region that are showing increasing or decreasing trends in sea surface temperature (SST) for each of the standard IGMETS time-windows. Numbers in brackets indicate the % area with significant ($p < 0.05$) trends. See "Methods" chapter for a complete description and methodology used.

Latitude-adjusted SST data field surface area = 46.1 million km²	**5-year** (2008–2012)	**10-year** (2003–2012)	**15-year** (1998–2012)	**20-year** (1993–2012)	**25-year** (1988–2012)	**30-year** (1983–2012)
Area (%) w/ increasing SST trends ($p < 0.05$)	**52.5%** (*13.3%*)	**50.3%** (*14.6%*)	**76.8%** (*54.8%*)	**95.7%** (*87.4%*)	**98.1%** (*95.0%*)	**99.1%** (*97.3%*)
Area (%) w/ decreasing SST trends ($p < 0.05$)	47.5% (*18.6%*)	49.7% (*15.5%*)	23.2% (*7.1%*)	4.3% (*1.1%*)	1.9% (*0.6%*)	0.9% (*0.3%*)
> 1.0°C decade^{-1} warming ($p < 0.05$)	13.5% (*8.1%*)	3.4% (*3.3%*)	0.9% (*0.9%*)	0.7% (*0.7%*)	0.1% (*0.1%*)	0.0% (*0.0%*)
0.5 to 1.0°C decade^{-1} warming ($p < 0.05$)	18.0% (*4.6%*)	5.0% (*4.1%*)	5.4% (*5.4%*)	10.0% (*10.0%*)	9.2% (*9.2%*)	6.7% (*6.7%*)
0.1 to 0.5°C decade^{-1} warming ($p < 0.05$)	17.0% (*0.6%*)	27.3% (*7.1%*)	**56.3%** (*47.4%*)	**77.1%** (*74.3%*)	**83.3%** (*82.5%*)	**86.7%** (*86.4%*)
0.0 to 0.1°C decade^{-1} warming ($p < 0.05$)	4.1% (*0.0%*)	14.6% (*0.2%*)	14.2% (*1.2%*)	8.0% (*2.4%*)	5.4% (*3.2%*)	5.6% (*4.2%*)
0.0 to –0.1°C decade^{-1} cooling ($p < 0.05$)	3.9% (*0.0%*)	13.1% (*0.1%*)	10.0% (*0.2%*)	2.6% (*0.1%*)	1.3% (*0.1%*)	0.7% (*0.1%*)
–0.1 to –0.5°C decade^{-1} cooling ($p < 0.05$)	13.3% (*0.7%*)	29.2% (*8.7%*)	12.4% (*6.1%*)	1.4% (*0.8%*)	0.6% (*0.4%*)	0.2% (*0.1%*)
–0.5 to –1.0°C decade^{-1} cooling ($p < 0.05$)	15.7% (*6.6%*)	6.7% (*6.1%*)	0.7% (*0.6%*)	0.2% (*0.2%*)	0.1% (*0.1%*)	0.0% (*0.0%*)
> –1.0°C decade^{-1} cooling ($p < 0.05$)	14.6% (*11.3%*)	0.6% (*0.6%*)	0.2% (*0.2%*)	0.0% (*0.0%*)	0.0% (*0.0%*)	0.0% (*0.0%*)

4.3 Trends from *in situ* time series

The North Atlantic is home to the largest fraction of *in situ* marine ecological time series globally, though most of them are clustered around continental margins, many in coastal waters (Table 4.3). The distribution of sites is also skewed to the temperate regions of the basin, with very few stations located in subtropical and tropical waters (Figure 4.4). Nevertheless, the data obtained still serve as an invaluable tool to examine the consistency between local and regional changes in environmental and plankton variables. Trends in *in situ* SST match well those derived by satellite. For the 10-year time-window, both *in situ* observations and gridded values showed almost an equivalent number of cases of increasing and decreasing trends (Table 4.2, Figure 4.5). This equivalence indicates that it is not possible to determine a regional coherent trend for this time-window, highlighting the importance of local heterogeneity in the responses of individual variables to climate.

The increasing SST trends tended to dominate in the 20- and 30-year analysis periods (Figure 4.5). Conversely, negative trends in oxygen and nutrients, as exemplified by nitrate, were more frequent over these time-windows. However, given the uneven distribution of *in situ* time series, no clear trend in chemical variables was evident at a basin-scale. For example, during 2003–2012, nitrate increased in most coastal locations across the Northeast Atlantic and in some locations in the northwest subbasin, such as the southern Bay of Biscay and Helgoland, while it decreased at some locations in the Baltic Sea and at the two sites available for the Mediterranean (Figure 4.4). Considering all the compiled time series, even those with shorter dataperiods, the number of series showing increasing trends in phytoplankton slightly exceeded those with decreasing trends, but particularly over long time windows (> 20 years; Figure 4.5). Sites with decreasing phytoplankton were

found in waters north of 50°N, in the southern Bay of Biscay and in the northern Mediterranean (Figure 4.4). Similarly, most sites recorded increases in diatoms (but not in dinoflagellates) in time-windows exceeding 20 years, but, conversely, dinoflagellates increased in periods < 10 years (Figure 4.5).

Consequently, the trends in the ratio diatom/dinoflagellate changed from negative to positive when extending the time-window from 5 to 30 years. Increasing trends in zooplankton also exceeded 50% of available time series over short time-windows (< 10 years), but their frequency decreased for time-windows > 10 years and even switched to a negative-trend dominance for some periods, suggesting an uncoupling with the trends in phytoplankton (Figure 4.5). During 2003–2012, sites with increasing zooplankton were sometimes associated with decreasing phytoplankton, as observed in ocean waters east of Greenland and in some locations on the continental shelf area south of Newfoundland, but there were also examples of zooplankton decreases and a concomitant increase in phytoplankton, e.g. along the coast of North America (Figure 4.4).

The asymmetry in the trends observed can be illustrated by comparing the differences among time series in the marginal seas, such as the Baltic and Mediterranean (Figures 2.6b,c). We will only consider the 5-year time-window (2008–2012) for this example because it contains the largest number of time series. Over this time-window, there was a clear dominance of positive trends in zooplankton and dinoflagellates for the North Atlantic basin as a whole (Figure 4.5a). For time series not included in marginal seas (Figure 4.6a), this pattern was not observed for oxygen, but still holds for zooplankton and dinoflagellates. In the Baltic, trends were mostly characterized by a cooling and decrease in phytoplankton, most notably diatoms (Figure 4.6b). Interestingly, the change in the phytoplankton community indicated by a decrease in the value of the diatom/dinoflagellate ratio was apparently similar in the North Atlantic proper and in the Baltic, but in the former case, the change

Table 4.2. Relative spatial areas (% of the total region) and rates of change within the North Atlantic region (including the Baltic Sea and Mediterranean Sea) that are showing increasing or decreasing trends in phytoplankton biomass (CHL) for each of the standard IGMETS time-windows. Numbers in brackets indicate the % area with significant ($p < 0.05$) trends. See "Methods" chapter for a complete description and methodology used.

Latitude-adjusted CHL data field surface area = 46.1 million km^2	**5-year** (2008–2012)	**10-year** (2003–2012)	**15-year** (1998–2012)
Area (%) w/ increasing CHL trends ($p < 0.05$)	30.2% (*3.6%*)	43.9% (*14.4%*)	38.0% (*12.7%*)
Area (%) w/ decreasing CHL trends ($p < 0.05$)	**69.8%** (*25.0%*)	**56.1%** (*28.2%*)	**62.0%** (*38.3%*)
> 0.50 mg m^{-3} decade^{-1} increasing ($p < 0.05$)	0.8% (*0.2%*)	1.2% (*1.0%*)	2.3% (*2.2%*)
0.10 to 0.50 mg m^{-3} decade^{-1} increasing ($p < 0.05$)	5.7% (*1.7%*)	6.3% (*4.5%*)	4.1% (*3.4%*)
0.01 to 0.10 mg m^{-3} decade^{-1} increasing ($p < 0.05$)	14.9% (*1.6%*)	17.8% (*6.8%*)	16.6% (*5.9%*)
0.00 to 0.01 mg m^{-3} decade^{-1} increasing ($p < 0.05$)	8.7% (*0.0%*)	18.5% (*2.2%*)	15.1% (*1.2%*)
0.00 to –0.01 mg m^{-3} decade^{-1} decreasing ($p < 0.05$)	11.0% (*0.4%*)	18.4% (*3.9%*)	30.4% (*15.3%*)
–0.01 to –0.10 mg m^{-3} decade^{-1} decreasing ($p < 0.05$)	40.8% (*15.0%*)	33.1% (*21.2%*)	30.5% (*22.3%*)
–0.10 to –0.50 mg m^{-3} decade^{-1} (decreasing) ($p < 0.05$)	13.5% (*6.6%*)	3.8% (*2.4%*)	1.0% (*0.7%*)
> –0.50 mg m^{-3} decade^{-1} (decreasing) ($p < 0.05$)	4.4% (*3.0%*)	0.9% (*0.7%*)	0.0% (*0.0%*)

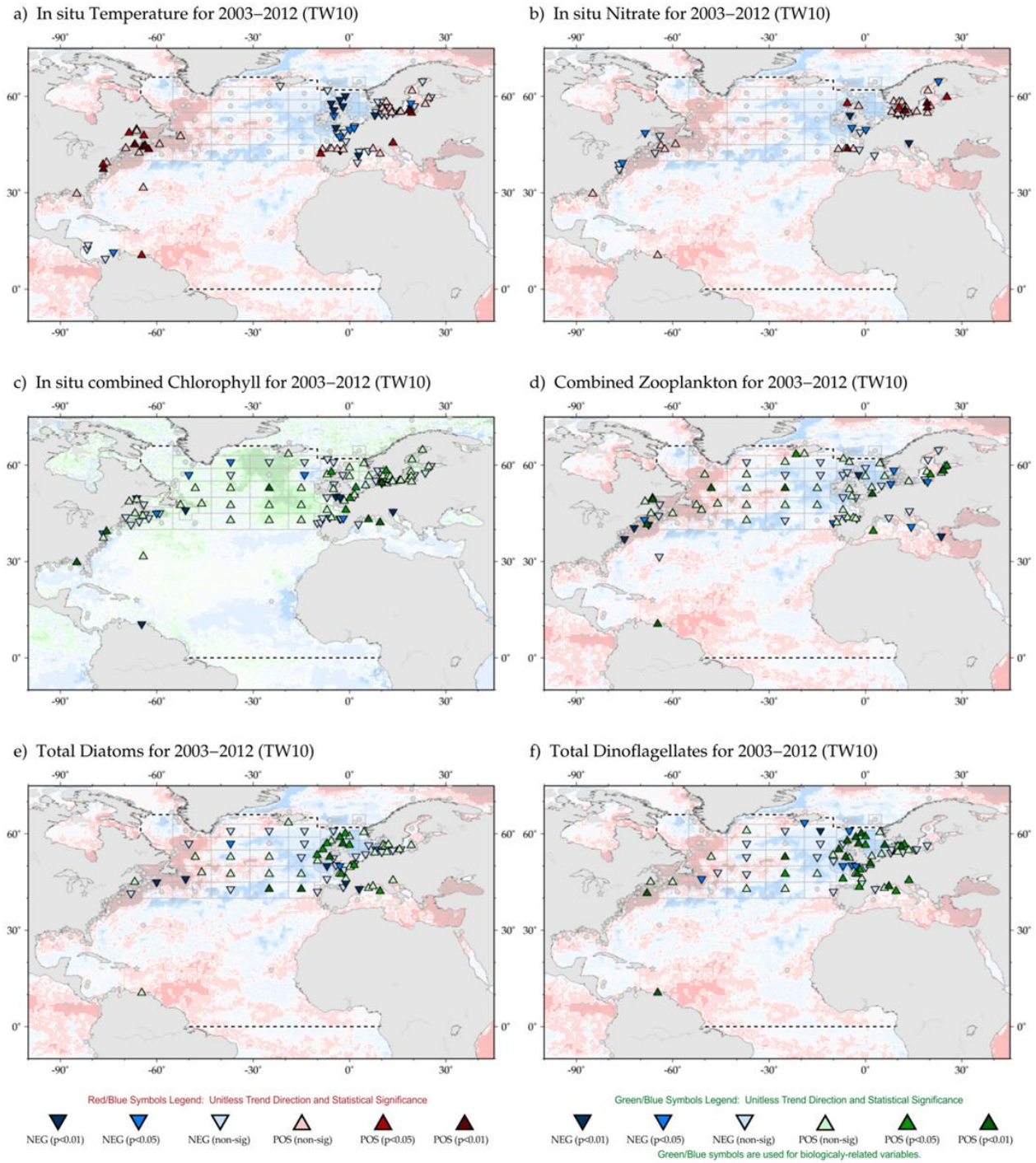

Figure 4.4. Map of North Atlantic region time-series locations and trends for select variables and IGMETS time-windows. Upward-pointing triangles indicate positive trends; downward triangles indicate negative trends. Gray circles indicate time-series site that fell outside of the current study region or time-window. Additional variables and time-windows are available through the IGMETS Explorer (http://IGMETS.net/explorer). See "Methods" chapter for a complete description and methodology used.

was due to an increase in dinoflagellates, while in the latter, it was caused by a decrease in diatoms. In contrast with the changes in the North Atlantic proper, the Mediterranean showed no change in SST, a decrease in nitrate, and an increase in all phytoplankton groups (Figure 4.6c). It is important to note that stations in the Mediterranean are located in coastal waters (see Figure 4.4), and these observations cannot be extrapolated to open Mediterranean waters.

A first examination of potential causal factors of these trends can be provided by the pairwise correlation of time-series, as exemplified for the 10-year time-window (Figure 4.7). Changes in Reynolds SST trends were well represented in nearly all *in situ* series, with a few exceptions (Figure 4.4). Over this 10-year time-window, only oxygen and dinoflagellates varied inversely with SST (Figure 4.7a).

In contrast, satellite-derived chlorophyll appeared more clearly associated with changes in *in situ* plankton variables, as shown by the positive correlations with phytoplankton and zooplankton series (Figure 4.7c). However, it is difficult to generalize about these relationships as there is large heterogeneity throughout the North Atlantic. For example, during 2003–2012, there was an equivalent number of marine ecological time series showing positive and negative correlations between some *in situ* phytoplankton variables (e.g. the abundance of diatoms or the diatom/dinoflagellate ratio) and satellite chlorophyll (Figure 4.7c), suggesting divergent changes in pigment content or cell size.

It must also be noted that only a small fraction of the correlations were significant (for more details, see the IGMETS Explorer), and that there are still large regions of the North Atlantic, particularly in subtropical and tropical regions, that were not covered by *in situ* time-series observations, as they do not exist or were not appropriate for the purpose of IGMETS. In addition, these correlations also vary at different time-scales, as indicated by the increase in the proportion of positive trends in most variables with increasing time-window (Figure 4.5).

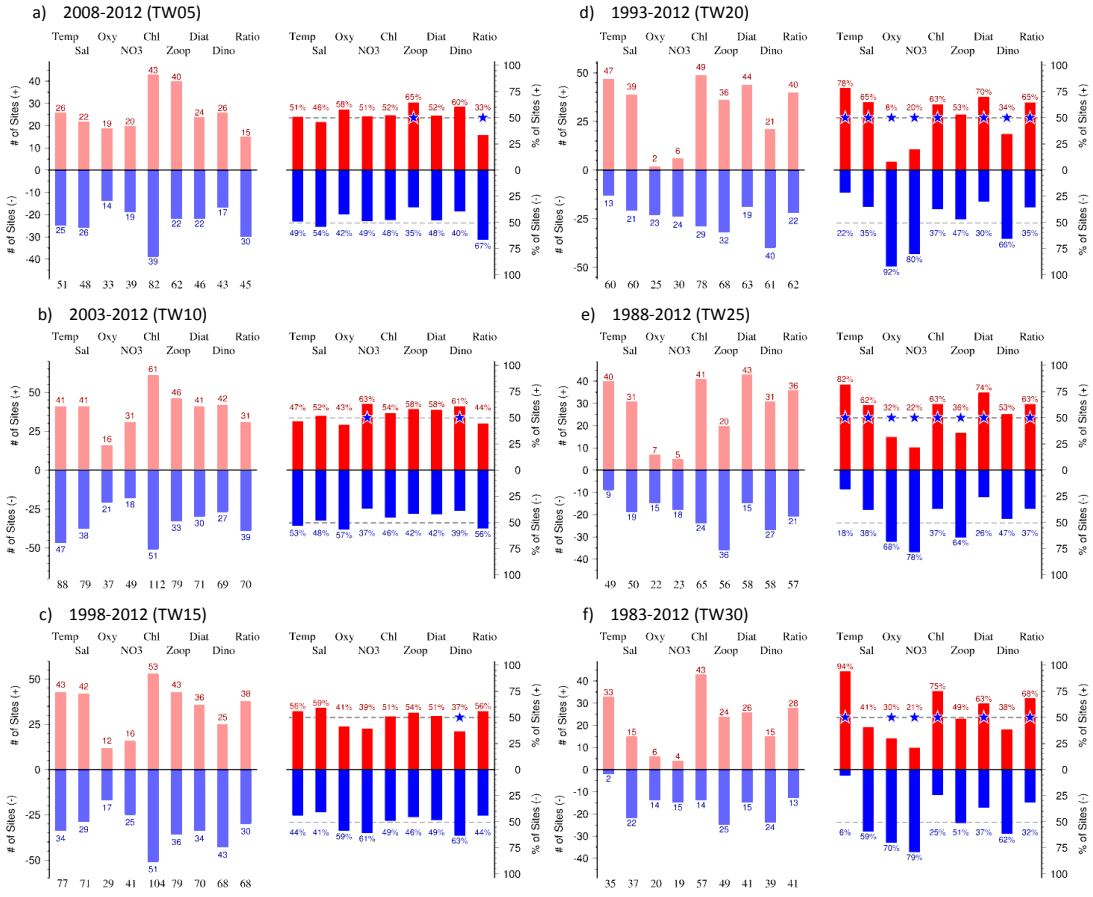

Figure 4.5. Absolute (left) and relative (%, right) frequency of positive and negative trends in selected variables from *in situ* time series in the North Atlantic region computed for different IGMETS time-windows. The 50% relative frequency is indicated by dashed lines in the right panels. A star symbol on this dashed line indicates that the trend was statistically different ($p < 0.05$) from 50%. See "Methods" chapter for a complete description and methodology used.

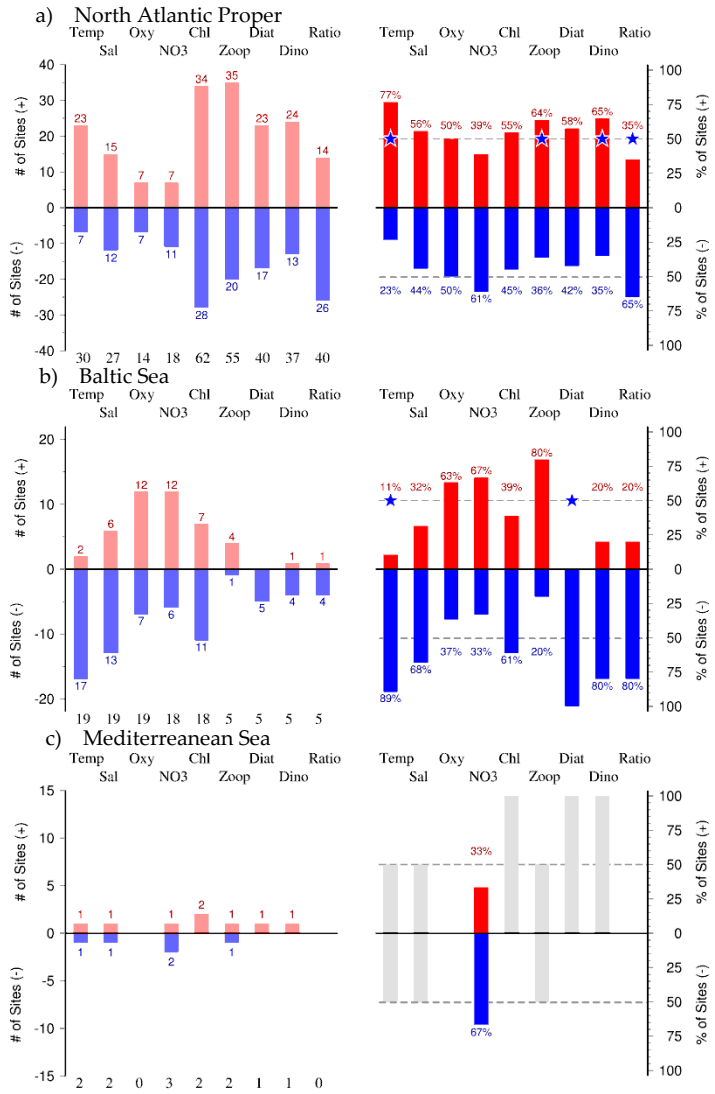

Figure 4.6. Absolute (left) and relative (%, right) frequency of positive and negative trends in variables from *in situ* time-series in the North Atlantic proper, a) excluding semi-enclosed seas, b) Baltic, and c) Mediterranean seas computed for a 5-year time-window. The 50% relative frequency is indicated by dashed lines in the right panels. See "Methods" chapter for a complete description and methodology used.

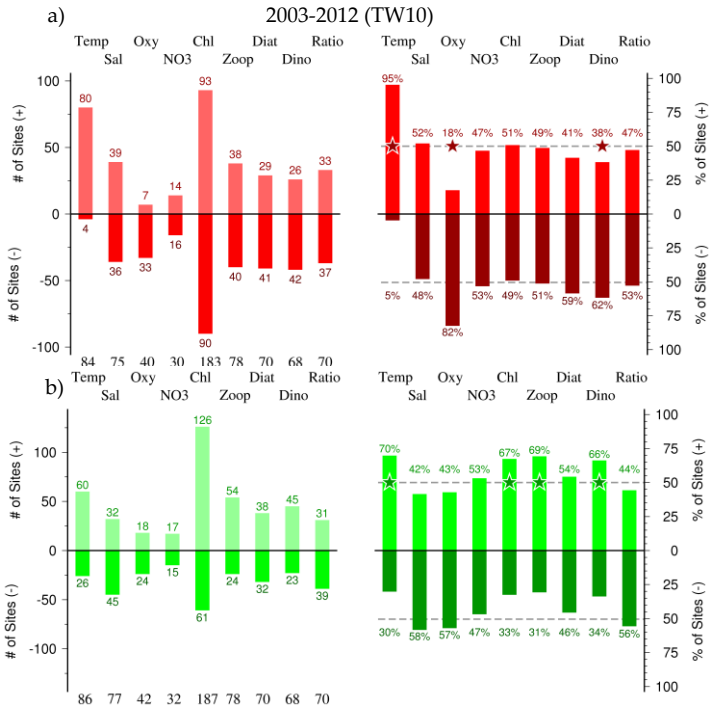

Figure 4.7. Absolute (left) and relative (%, right) frequency of positive and negative correlations between selected *in situ* North Atlantic time-series variables and corresponding gridded SST (red bars – a) and chlorophyll (green bars – b) for the 10-year time-window (2002–2012). The 50% relative frequency is indicated by dashed lines in the right panels. A star symbol on this dashed line indicates that the trend was statistically different ($p < 0.05$) from 50%. See "Methods" chapter for a complete description and methodology used.

4.4 Consistency with previous analysis

Previous analyses of trends in oceanographic variables over the North Atlantic, some using time-series data collected by IGMETS, already showed some of the changes illustrated here. The increasing warming trends in the North Atlantic are some of the most repeated examples of global change in the ocean (Levitus *et al*., 2000; Hoegh-Guldberg *et al*., 2014). These changes were related to various climate forcings over the North Atlantic basin, highlighting the role of multidecadal oscillations and other natural phenomena (Hurrell *et al*., 2009; Knudsen *et al*., 2011). There is evidence that spring blooms initiated later than average in the mid-1980s, but earlier in the 1990s due to fluctuations in the NAO over the central North Atlantic (Zhai *et al*., 2013). Different trends in SST are expected, driven by changes in upwelling intensity along the eastern margin of the North Atlantic (the Canary–Iberian upwelling system). Some authors indicate that upwelling in this region is either decreasing (Pardo *et al*., 2011, Santos *et al*., 2012) or increasing (McGregor *et al*., 2007). Benazzouz *et al*. (2015) suggest that, in contrast to other upwelling regions, recent increases in wind intensity in the Canary–Iberian upwelling system may lead to upwelling of warm waters at the regional level, and at the same time, this may allow for an increase in local primary production (Demarcq and Benazzouz, 2015). The divergent trends in SST and other variables observed in local time series in the southern Bay of Biscay (Figure 4.4) may be an indication of small-scale interaction between regional and local factors. More long-term ecological observations along the subtropical eastern North Atlantic are needed in order to improve the analysis of changes in upwelling and their consequences for ecosystems.

Large changes in North Atlantic ecosystems resulted in regime shifts over long time-periods. The regime shifts that occurred in the North Sea and adjacent regions were well studied, as the consequences affected many ecosystem components (McQuatters-Gollop *et al*., 2007; Reid *et al*., 2010; Beaugrand *et al*., 2015). There were also regime shifts identified in other regions both in the eastern (Hatun *et al*., 2009) and western basins (Plourde *et al*., 2014; Meyer-Gutbrod *et al*., 2015) that affected plankton and also upper trophic-level consumers. While the time-window approach selected in this first IGMETS analysisi is not well suited to identify regime shifts, the large intraregional variability in these regime shifts calls for more comparative analysis to understand the scale-dependent dynamics of climate effects (Fisher *et al*., 2015). Changes in nutrient inputs were addressed mainly as consequence of oceanographic variability in water masses and anthropogenic inputs (Llope *et al*., 2007; Heath and Beare, 2008; Pérez *et al*., 2010), often with divergent trends that were difficult to untangle without a good geographic distribution of *in situ* observations.

The general decrease observed in satellite chlorophyll in the North Atlantic (Table 4.1) has already been noted in previous studies (Boyce *et al*., 2014). Behrenfeld *et al*. (2015) suggested that this may result from physiological adaptations related to thermal stratification rather than a true decrease in primary production. There are areas that exhibit an increase in satellite chlorophyll (e.g. most of the non-subtropical North Atlantic and subarctic waters). Local series of coastal phytoplankton biomass often reflect the interaction of several factors, as exemplified in the study of the effects of wind and water temperature on nutrient replenishment and phytoplankton dynamics during the winter– spring period between 1979 and 2011 in the northern Mediterranean (Goffart *et al*., 2015). Analysis of primary production observations has pointed out the large heterogeneity in local responses (Bode *et al*., 2011), and several studies have also shown a shift in the relative dominance of diatoms, dinoflagellates, and other phyotplankton groups (Leterme *et al*., 2006; O'Brien *et al*., 2012; Suikkanen *et al*., 2013). Recently, underlying changes at the species-specific level have been highlighted, which ultimately affect the composition of phytoplankton communities (Hinder *et al*., 2012; Bode *et al*., 2015). These observations stress the value and need of *in situ* marine ecological time series; most of the changes observed have been identified by using detailed species composition, data than can only be provided by *in situ* time series.

While the long-term (30-year time-window) trends presented in this study are in general agreement with results from previous studies using remote sensing data, time-series measurements from individual stations as well as climatological fields, the interpretation of patterns observed with the selected time-windows must be made with caution. For example, the Baltic Sea shows long-term trends in increasing water temperatures (i.e. warming), decreasing oxygen (i.e. deoxygenation), and decreasing nitrate (i.e. reduced eutrophication). However, the results for the 5-year time-window (Figure 4.6) reveal a statistically significant majority of trends with opposite signs for water temperature and oxygen concentrations, which, in turn, imply cooling and increasing

oxygen concentrations during 2008–2012. These apparent differences between short- and long-term trends can be attributed to the choice of time-window and, of course, do not imply regime shifts and reversals of the observed long-term trends.

Similarly, direct comparison of trends in concurrently measured variables may lead to misinterpretations. Time-series measurements of nitrate in the surface layer of the Baltic Sea show maximum concentrations during the late 1980s, but the input of nitrate to the Baltic Sea has subsequently been reduced drastically and has resulted in a significant decrease in nitrate surface concentrations in some basins (Feistel *et al*., 2008; HELCOM, 2009, 2014). However, chlorophyll *a* trends still show no signs of decrease or have even increased in recent years in some Baltic Sea basins. The long residence time of water as well as phosphorus release from anoxic sediments in combination with blooms of nitrogen fixing cyanobacteria have been identified as slowing the decrease in eutrophication in the Baltic Proper. The obvious paradox of ongoing oxygen loss despite decreasing eutrophication in the coastal regions of the Baltic Sea has been attributed to warming-induced enhanced organic matter respiration in combination with an extended period of water-column stratification (Lennartz *et al*., 2014). In contrast, Carstensen *et al*. (2014) showed that ongoing eutrophication is still the main reason for the observed long-term trend in enhanced oxygen loss in the deep basins of the Baltic Proper.

The effects of climate and oceanographic changes in temperature and circulation affecting nutrient inputs and displacement of plankton are more difficult to trace through the foodweb, as there is a mixture of direct and indirect effects affecting the different trophic levels. This can cause mismatches between observed trends, such as those of phytoplankton and zooplankton at different time-windows (Figure 4.4) and shown by previous studies (Richardson and Schoeman, 2004; McGinty *et al*., 2012).

4.5 Conclusions

The first comprehensive analysis of *in situ* time series provided by IGMETS in the North Atlantic revealed that, despite being the most studied region of the global ocean, there are large areas in this region still not covered by multidisciplinary *in situ* observations. Most of the time series are located in areas very close to the coasts; even in regions well covered by regular observations, such as north of the subtropical gyre, there is no physical (e.g. temperature, salinity) or chemical (e.g. oxygen, nutrients) information to match the biological data. The analysis of existing time series revealed that, even in adjacent areas that appear to be relatively homogenous, there is large variability in ecosystem behaviour over time as observed in the continental shelves at both sides of the North Atlantic.

Table 4.3 Time-series sites located in the IGMETS North Atlantic (not including Baltic Sea and Mediterranean Sea) region. Participating countries: Canada (ca), Colombia (co), Germany (de), Denmark (dk), Spain (es), Faroe Islands (fo), France (fr), Ireland (ie), Isle of Man (im), Iceland (is), Norway (no), Portugal (pt), United Kingdom (uk), United States (us), and Venezuela (ve). Year-spans in red text indicate time series of unknown or discontinued status. IGMETS-IDs in red text indicate time series without a description entry in Annex 2.

No.	IGMETS-ID	Site or programme name	Year-span	T	S	Oxy	Ntr	Chl	Mic	Phy	Zoo
1	ca-50101	AZMP Halifax Line 2 *(Scotian Shelf)*	1997–present	X	-	-	-	X	-	-	X
2	ca-50102	AZMP Prince 5 *(Bay of Fundy)*	1999–present	X	-	-	-	X	-	-	X
3	ca-50201	AR7W Zone 1 *(Labrador Shelf)*	1996–present	X	X	-	-	X	-	-	X
4	ca-50202	AR7W Zone 2 *(Labrador Slope)*	1996–present	X	X	-	-	X	-	-	X
5	ca-50203	AR7W Zone 3 *(Central Labrador Sea)*	1996–present	X	X	-	-	X	-	-	X
6	ca-50204	AR7W Zone 4 *(Eastern Labrador Sea)*	1996–present	X	X	-	-	X	-	-	X
7	ca-50205	AR7W Zone 5 *(Greenland Shelf)*	1996–present	X	X	-	-	X	-	-	X
8	ca-50401	Bedford Basin *(Northwestern North Atlantic)*	1967–present	X	X	-	X	X	X	-	-
9	ca-50501	Bay of Fundy *(Northwestern Atlantic shelf)*	1988–2012 discontinued	X	X	-	-	X	-	X	-
10	ca-50601	AZMP Station 27 *(Newfoundland Shelf)*	1960–present	X	-	-	-	X	-	-	X
11	ca-50701	AZMP Anticosti Gyre *(Gulf of St Lawrence)*	1999–present	X	-	-	-	X	-	-	X
12	ca-50702	AZMP Gaspe Current *(Gulf of St Lawrence)*	1999–present	X	-	-	-	X	-	-	X
13	ca-50703	AZMP Rimouski *(Gulf of St Lawrence)*	2005–present	X	X	-	X	X	-	-	X
14	ca-50704	AZMP Shediac *(Gulf of St Lawrence)*	1999–present	X	X	-	X	X	-	-	X
15	ca-50801	Central Scotian Shelf *(Northwestern Atlantic shelf)*	1996–present	X	X	-	X	X	X	-	-
16	ca-50802	Eastern Scotian Shelf *(Northwestern Atlantic)*	1997–present	X	X	-	X	X	X	-	-
17	ca-50803	Western Scotian Shelf *(Northwestern Atlantic)*	1997–present	X	X	-	X	X	X	-	-
18	co-30101	REDCAM Isla de San Andres *(Southwestern Caribbean)*	2002–present	X	X	X	-	-	-	-	-
19	co-30102	REDCAM Isla de Provencia *(Southwestern Caribbean)*	2002–present	X	X	X	-	-	-	-	-

No.	IGMETS-ID	Site or programme name	Year-span	T	S	Oxy	Ntr	Chl	Mic	Phy	Zoo
20	co-30103	REDCAM Western Colombia–Caribbean Shelf *(Southwestern Caribbean)*	2002–present	X	X	X	-	-	-	-	-
21	co-30104	REDCAM Eastern Colombia–Caribbean Shelf *(Southwestern Caribbean)*	2002–present	X	X	X	-	-	-	-	-
22	de-10101	Nordeney WQ-W2 *(Southern North Sea)*	1999–2008 (?)	X	X	-	X	-	-	X	-
23	de-30201	Helgoland Roads *(Southeastern North Sea)*	1962–present	X	X	-	X	-	X	X	X
24	de-30301	Cape Verde Ocean Observatory *(Tropical Eastern North Atlantic)*	2006–present	X	X	X	X	-	-	-	-
27	dk-30101	North Sea: DNAMAP-1510007 *(Baltic Sea)* *see Baltic Sea Annex (A2)*	1989–present	X	X	X	X	X	-	X	-
28	dk-30105	Ringkobing Fjord: DNAMAP-1 *(Baltic Sea)* *see Baltic Sea Annex (A2)*	1980–present	X	X	X	X	X	-	X	-
29	dk-30106	Nissum Fjord: DNAMAP-22 *(Baltic Sea)* *see Baltic Sea Annex (A2)*	1983–present	X	X	X	X	X	-	X	-
30	dk-30107	Nissum Bredning: DNAMAP-3702-1 *(Baltic Sea)* *see Baltic Sea Annex (A2)*	1982–present	X	X	X	X	X	-	X	-
31	dk-30110	Lister Dyb: DNAMAP-3 *(Baltic Sea)* *see Baltic Sea Annex (A2)*	1993–present	X	X	X	X	X	-	X	-
32	es-30101	BILBAO 35 Time Series *(Inner Bay of Biscay)*	1998–present	X	X	X	-	X	-	-	X
33	es-30102	URDAIBAI 35 Time Series *(Inner Bay of Biscay)*	1997–present	X	Xs	X	-	X	-	-	X
34	es-30201	AZTI Station D2 *(Southeastern Bay of Biscay)*	1986–present	X	X	X	X	X	-	X	-
35	es-30401	Nervion River Estuary E1 *(Southern Bay of Biscay)*	2000–present	X	X	-	-	-	-	X	-
36	es-50101	RADIALES Santander Station 4 *(Southern Bay of Biscay)*	1991–present	X	X	*	X	*	*	-	X
37	es-50102	RADIALES A Coruna Station 2 *(Northwestern Iberian coast)*	1988–present	X	X	X	X	X	X	X	X
38	es-50103	RADIALES Gijon/Xixon Station 2 *(Southern Bay of Biscay)*	2001–present	X	X	*	X	X	X	X	X
39	es-50104	RADIALES Vigo Station 3 *(Northwest Iberian coast)*	1994–present	X	X	-	X	X	-	-	X
40	es-50105	RADIALES Cudillero Station 2 *(Southern Bay of Biscay)*	1992–present	X	X	X	X	X	*	-	X

No.	IGMETS-ID	Site or programme name	Year-span	T	S	Oxy	Ntr	Chl	Mic	Phy	Zoo
41	fo-30101	Faroe Islands Shelf *(Faroe Islands)*	1991–present	X	-	-	X	X	-	-	X
42	fr-50101	REPHY Antifer Ponton Petrolier *(English Channel)*	1989–present	X	X	X	X	X	-	X	-
43	fr-50102	REPHY At So *(English Channel)*	1987–present	X	X	-	X	X	-	X	-
44	fr-50103	REPHY Donville *(English Channel)*	2002–present	X	X	X	X	X	-	X	-
45	fr-50104	REPHY Pen al Lann *(English Channel)*	1987–present	X	X	X	-	X	-	X	-
46	fr-50105	REPHY Point 1 SRN Boulogne *(English Channel)*	1992–present	X	X	-	X	X	-	X	-
47	fr-50106	REPHY Kervel *(Bay of Biscay)*	1987–present	X	X	-	-	X	-	X	-
48	fr-50107	REPHY Le Cornard *(Bay of Biscay)*	1987–present	X	X	X	-	X	-	X	-
49	fr-50108	REPHY Men er Roue *(Bay of Biscay)*	1987–present	X	X	-	X	X	-	X	-
50	fr-50109	REPHY Ouest Loscolo *(Bay of Biscay)*	1987–present	X	X	-	X	X	-	X	-
51	fr-50110	REPHY Teychan Bis *(Bay of Biscay)*	1999–present	X	X	-	X	X	-	X	-
52	fr-50201	Gravelines Station *(English Channel)*	1993–present	-	-	-	-	-	-	-	X
53	ie-30101	East Coast Ireland *(Ireland)*	1990–present	-	-	-	-	-	-	X	-
54	ie-30102	Northwest Coast Ireland *(Ireland)*	1990–present	-	-	-	-	-	-	X	-
55	ie-30103	South Coast Ireland *(Ireland)*	1990–present	-	-	-	-	-	-	X	-
56	ie-30104	Southwest Coast Ireland *(Ireland)*	1990–present	-	-	-	-	-	-	X	-
57	ie-30105	West Coast Ireland (*Ireland*)	1990–present	-	-	-	-	-	-	X	-
58	im-10101	Cypris Station – Isle of Man *(Irish Sea)*	1954–2009 (?)	X	X	X	X	X	-	X	-
59	is-30102	Selvogsbanki Transect *(South Iceland)*	1971–present	X	X	-	-	X	-	-	X
60	no-50401	Arendal Station 2 *(North Sea)*	1994 – present	X	X	X	X	X	-	-	X
61	pt-30101	Cascais Bay *(Portuguese Coast)*	2005–present	X	X	-	-	-	-	-	X

No.	IGMETS-ID	Site or programme name	Year-span	T	S	Oxy	Ntr	Chl	Mic	Phy	Zoo
62	pt-30201	Guadiana Lower Estuary *(Southwest Iberian Peninsula)*	1996–present	X	X	-	-	X	-	-	X
63	pt-30301	Guadiana Upper Estuary *(Southwest Iberian Peninsula)*	1996–present	X	X	-	X	X	X	X	-
64	uk-30101	Stonehaven *(Northwest North Sea)*	1997–present	X	X	-	X	X	-	X	X
65	uk-30102	Loch Ewe *(West coast Scotland)*	2002–present	X	X	-	X	X	-	X	X
66	uk-30103	Loch Maddy *(West coast Scotland)*	2003–2011 (?)	X	X	-	X	-	-	X	-
67	uk-30104	Mill Port *(West coast Scotland)*	2005–2013 (?)	X	-	-	-	-	-	X	-
68	uk-30105	Scalloway – Shetland Isles *(Northwest North Sea)*	2001–present	X	X	-	X	-	-	X	-
69	uk-30106	Scapa Bay – Orkney *(Northwest North Sea)*	2001–present	X	X	-	X	-	-	X	-
70	uk-30201	Plymouth L4 *(Western English Channel)*	1988–present	X	X	X	X	X	X	X	X
71	uk-30301	Dove *(North Sea)*	1971–2002 discontinued	-	-	-	-	-	-	-	X
72	uk-30601	Atlantic Meridional Transect (AMT)	1995-present	X	X	X	X	X		X	X
73	uk-40106	SAHFOS–CPR A06 *(South Iceland)*	1958–present	-	-	-	-	X	-	X	X
74	uk-40111	SAHFOS–CPR B01 *(Northeastern North Sea)*	1958–present	-	-	-	-	X	-	X	X
75	uk-40112	SAHFOS–CPR B02 *(Northwestern North Sea)*	1958–present	-	-	-	-	X	-	X	X
76	uk-40114	SAHFOS–CPR B04 *(Southern Norwegian Sea)*	1958–present	-	-	-	-	X	-	X	X
77	uk-40115	SAHFOS–CPR B05 *(Southeast Iceland)*	1958–present	-	-	-	-	X	-	X	X
78	uk-40116	SAHFOS–CPR B06 *(Southwest Iceland)*	1958–present	-	-	-	-	X	-	X	X
79	uk-40117	SAHFOS–CPR B07 *(Southeast Greenland)*	1958–present	-	-	-	-	X	-	X	X
80	uk-40118	SAHFOS–CPR B08 *(Southwest Greenland)*	1962–present	-	-	-	-	X	-	X	X
81	uk-40121	SAHFOS–CPR C01 *(Eastern Central North Sea)*	1958–present	-	-	-	-	X	-	X	X
82	uk-40122	SAHFOS–CPR C02 *(Western Central North Sea)*	1958–present	-	-	-	-	X	-	X	X

No.	IGMETS-ID	Site or programme name	Year-span	T	S	Oxy	Ntr	Chl	Mic	Phy	Zoo
83	uk-40123	SAHFOS–CPR C03 *(Irish Sea)*	1958–present	-	-	-	-	X	-	X	X
84	uk-40124	SAHFOS–CPR C04 *(Northwest Scotland and Ireland)*	1958–present	-	-	-	-	X	-	X	X
85	uk-40125	SAHFOS–CPR C05 *(Northeast Central North Atlantic)*	1958–present	-	-	-	-	X	-	X	X
86	uk-40126	SAHFOS–CPR C06 *(Central North Atlantic)*	1958–present	-	-	-	-	X	-	X	X
87	uk-40127	SAHFOS–CPR C07 *(Northwest Central North Atlantic)*	1959–present	-	-	-	-	X	-	X	X
88	uk-40128	SAHFOS–CPR C08 *(Labrador)*	1959–present	-	-	-	-	X	-	X	X
89	uk-40131	SAHFOS–CPR D01 *(Southeast North Sea)*	1958–present	-	-	-	-	X	-	X	X
90	uk-40132	SAHFOS–CPR D02 *(Southwest North Sea)*	1958–present	-	-	-	-	X	-	X	X
91	uk-40133	SAHFOS–CPR D03 *(English Channel)*	1958–present	-	-	-	-	X	-	X	X
92	uk-40134	SAHFOS–CPR D04 *(South Ireland)*	1958–present	-	-	-	-	X	-	X	X
93	uk-40135	SAHFOS–CPR D05 *(Eastern Central North Atlantic)*	1958–present	-	-	-	-	X	-	X	X
94	uk-40136	SAHFOS–CPR D06 *(Central North Atlantic)*	1958–present	-	-	-	-	X	-	X	X
95	uk-40137	SAHFOS–CPR D07 *(Western Central North Atlantic)*	1959–present	-	-	-	-	X	-	X	X
96	uk-40138	SAHFOS–CPR D08 *(Western Central North Atlantic)*	1959–present	-	-	-	-	X	-	X	X
97	uk-40139	SAHFOS–CPR D09 *(Labrador Shelf)*	1959–present	-	-	-	-	X	-	X	X
98	uk-40144	SAHFOS–CPR E04 *(Bay of Biscay)*	1958–present	-	-	-	-	X	-	X	X
99	uk-40145	SAHFOS–CPR E05 (*Eastern Southern North Atlantic*)	1958–present	-	-	-	-	X	-	X	X
100	uk-40146	SAHFOS–CPR E06 (*Southern North Atlantic*)	1961–present	-	-	-	-	X	-	X	X
101	uk-40147	SAHFOS–CPR E07 (*Southern North Atlantic*)	1961–present	-	-	-	-	X	-	X	X
102	uk-40148	SAHFOS–CPR E08 (*Western Southern North Atlantic*)	1960–present	-	-	-	-	X	-	X	X
103	uk-40149	SAHFOS–CPR E09 (*Off Newfoundland Shelf*)	1960–present	-	-	-	-	X	-	X	X

No.	IGMETS-ID	Site or programme name	Year-span	T	S	Oxy	Ntr	Chl	Mic	Phy	Zoo
104	uk-40150	SAHFOS–CPR E10 (*Off Scotian Shelf*)	1961–present	-	-	-	-	X	-	X	X
105	uk-40154	SAHFOS–CPR F04 (*Off Iberian Shelf*)	1958–present	-	-	-	-	X	-	X	X
106	uk-40155	SAHFOS–CPR F05 (*Eastern Southern North Atlantic*)	1963–present	-	-	-	-	X	-	X	X
107	uk-40156	SAHFOS–CPR F06 (*Central Southern North Atlantic*)	1967–present	-	-	-	-	X	-	X	X
108	uk-40157	SAHFOS–CPR F07 (*Central Southern North Atlantic*)	1963–present	-	-	-	-	X	-	X	X
109	uk-40158	SAHFOS–CPR F08 (*Central Southern North Atlantic*)	1963–present	-	-	-	-	X	-	X	X
110	uk-40159	SAHFOS–CPR F09 (*Western Southern North Atlantic*)	1962–present	-	-	-	-	X	-	X	X
111	uk-40160	SAHFOS–CPR F10 (*Off Gulf of Maine*)	1961–present	-	-	-	-	X	-	X	X
112	us-10101	Bermuda Atlantic Time Series (*BATS*)	1982–present	X	X	X	X	X	X	-	X
113	us-10401	Boothbay (*Northwestern Atlantic shelf*)	2000–present	X	X	-	-	X	X	-	-
114	us-30101	Upper Chesapeake – Maryland (*Chesapeake Bay*)	1984–2002 (?)	-	-	-	-	-	-	-	X
115	us-30102	Lower Chesapeake – Virginia (*Chesapeake Bay*)	1985–2002 (?)	-	-	-	-	-	-	-	X
116	us-30201	Narragansett Bay (*Northwestern Atlantic*)	1959–present	X	X	-	X	X	-	-	-
117	us-30301	Neuse River Estuary NR000 (*Outer Banks – North Carolina*)	1994–present	X	X	X	X	X	-	-	-
118	us-30302	Pamlico Sound PS1 (*Outer Banks – North Carolina*)	2000–present	X	X	X	X	X	-	-	-
119	us-50101	EcoMon Gulf of Maine – GOM (*Gulf of Maine*)	1977–present	-	-	-	-	-	-	-	X
120	us-50102	EcoMon Georges Bank – GBK (*Georges Bank*)	1977–present	-	-	-	-	-	-	-	X
121	us-50103	EcoMon Southern New England – SNE (*Southern New England*)	1977–present	-	-	-	-	-	-	-	X
122	us-50104	EcoMon Mid-Atlantic Bight – MAB (*Mid-Atlantic Bight*)	1977–present	-	-	-	-	-	-	-	X
123	us-50105	EcoMon Gulf of Maine CPR line (*Gulf of Maine*)	1961–2012 discontinued	-	-	-	-	-	-	-	-
124	us-50106	EcoMon Mid-Atlantic Bight CPR line (*Mid-Atlantic Bight*)	1975–2012 discontinued	-	-	-	-	-	-	-	-

No.	IGMETS-ID	Site or programme name	Year-span	T	S	Oxy	Ntr	Chl	Mic	Phy	Zoo
125	us-50201	SEAMAP: Texas/Lousiana Shelf WEST (*Gulf of Mexico*)	1982–present	-	-	-	-	-	-	-	X
126	us-50202	SEAMAP: Texas/Louisiana Shelf CENTRAL (*Gulf of Mexico*)	1982–present	-	-	-	-	-	-	-	X
127	us-50203	SEAMAP: Texas/Lousiana Shelf EAST (*Gulf of Mexico*)	1982–present	-	-	-	-	-	-	-	X
128	us-50204	SEAMAP: Mississippi/Alabama Shelf (*Gulf of Mexico*)	1982–present	-	-	-	-	-	-	-	X
129	us-50205	SEAMAP: Florida Shelf NORTH-WEST (*Gulf of Mexico*)	1986–present	-	-	-	-	-	-	-	X
130	us-50206	SEAMAP: Florida Shelf NORTH-EAST (*Gulf of Mexico*)	1986–present	-	-	-	-	-	-	-	X
131	us-50207	SEAMAP: Florida Shelf SOUTH (*Gulf of Mexico*)	1982–present	-	-	-	-	-	-	-	X
132	us-50208	Northeast Off-shelf Region – SEAMAP (*Gulf of Mexico*)	1982–present	-	-	-	-	-	-	-	X
133	us-50209	Northwest Off-Shelf Region – SEAMAP (*Gulf of Mexico*)	1982–present	-	-	-	-	-	-	-	X
134	us-60101	NERRS ACE Basin	2001–present	X	X	X	X	X	-	-	-
135	us-60102	NERRS Apalachicola	2002–present	X	X	X	X	X	-	-	-
136	us-60103	NERRS Chesapeake Bay MD	2003–present	X	X	X	X	X	-	-	-
137	us-60104	NERRS Chesapeake Bay VA	2002–present	X	X	X	X	X	-	-	-
138	us-60105	NERRS Delaware	2001–present	X	X	X	X	X	-	-	-
139	us-60107	NERRS Grand Bay	2004–present	X	X	X	X	X	-	-	-
140	us-60108	NERRS Great Bay	2001–present	X	X	X	X	X	-	-	-
141	us-60109	NERRS Guana Tolomato Matanzas	2002–present	X	X	X	X	X	-	-	-
142	us-60111	NERRS Jacques Cousteau	2002–present	X	X	X	X	X	-	-	-
143	us-60112	NERRS Jobos Bay – Puerto Rico	2001–present	X	X	X	X	X	-	-	-
144	us-60115	NERRS Mission-Aransas	2007–present	X	X	X	X	X	-	-	-

No.	IGMETS-ID	Site or programme name	Year-span	T	S	Oxy	Ntr	Chl	Mic	Phy	Zoo
145	us-60116	NERRS Narragansett Bay	2002–present	X	X	X	X	X	-	-	-
146	us-60117	NERRS North Inlet – Winyah Bay	2001–present	X	X	X	X	X	-	-	-
147	us-60118	NERRS North Carolina	2001–present	X	X	X	X	X	-	-	-
148	us-60119	NERRS Old Woman Creek	2002–present	X	X	X	X	X	-	-	-
149	us-60121	NERRS Rookery Bay	2002–present	X	X	X	X	X	-	-	-
150	us-60122	NERRS Sapelo Island	2004–present	X	X	X	X	X	-	-	-
151	us-60126	NERRS Wells	2004–present	X	X	X	X	X	-	-	-
152	us-60127	NERRS Weeks Bay	2001–present	X	X	X	X	X	-	-	-
153	us-60128	NERRS Waquoit Bay	2002–present	X	X	X	X	X	-	-	-
154	ve-10101	CARIACO Ocean Time Series (*Cariaco Basin off Venezuela*)	1995–present	X	X	X	X	X	X	X	X

Baltic Sea

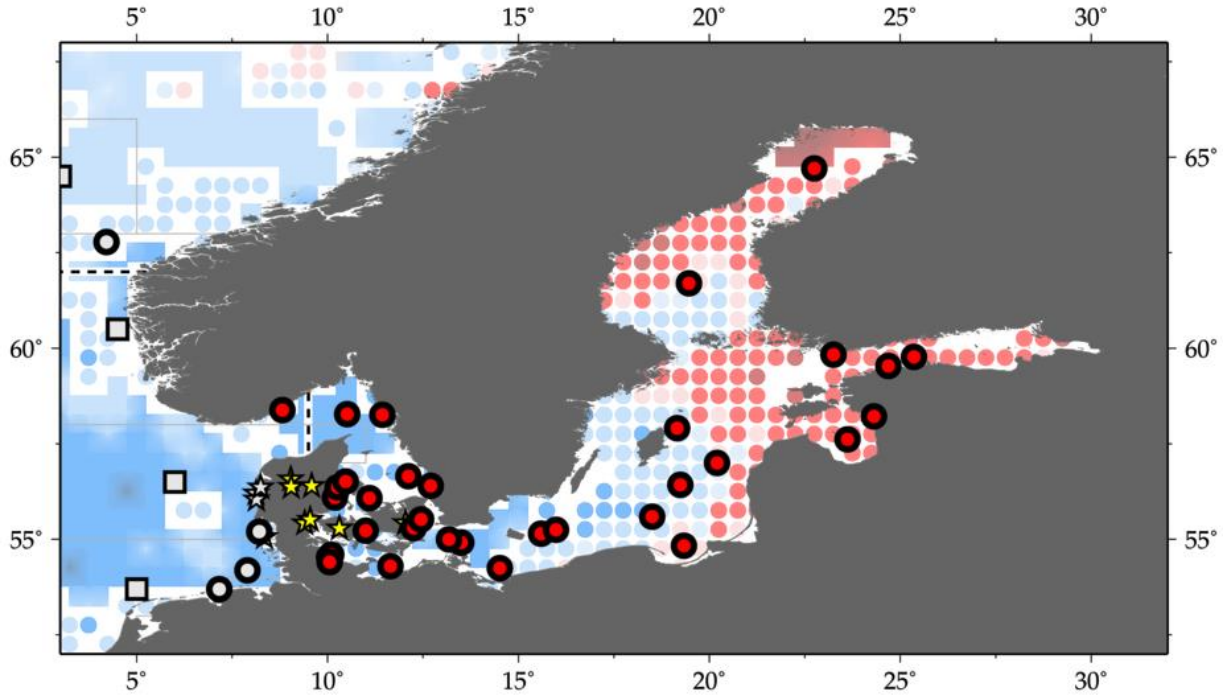

Figure 4.8. Map of IGMETS-participating Baltic Sea time series on a background of a 10-year time-window (2003–2012) sea surface temperature trends. At the time of this report, the Baltic Sea consisted of 41 time series (coloured symbols of any type, see also Table 4.4), of which 7 were from estuarine areas (yellow stars). Uncoloured (gray) symbols indicate time series being addressed in a different regional chapter (e.g. Arctic Ocean) or in separate subregions (e.g. North Atlantic Proper, Figure 4.1/Table 4.3; Mediterranean Sea, Figure 4.9/Table 4.5).

Table 4.4. Regional listing of participating time series for the IGMETS Baltic Sea. Participating countries: Germany (de), Denmark (dk), Estonia (ee), Finland (fi), Latvia (lv), Poland (pl), and Sweden (se).

No.	IGMETS-ID	Site or programme name	Year-span	T	S	Oxy	Ntr	Chl	Mic	Phy	Zoo
1	de-10201	Boknis Eck Time Series Station *(Eckernfoerde Bay – SW Baltic Sea)*	1957–present	X	X	X	X	X	X	-	-
2	de-30101	Arkona Basin (*Southern Baltic Sea*)	1979–present	X	X	X	X	X	X	X	X
3	de-30102	Bornholm Basin (*Southern Baltic Sea*)	1979–present	X	X	X	X	X	X	X	-
4	de-30103	Mecklenburg Bight (*Southern Baltic Sea*)	1980–present	X	X	X	X	X	X	X	-
5	de-30104	Eastern Gotland Basin (*Southern Baltic Sea*)	1979–present	X	X	X	X	X	X	X	-
6	dk-30102	Arhus Bugt: DNAMAP-170006 (*Baltic Sea*)	1979–present	X	X	X	X	X	-	X	-
7	dk-30103	Koge Bugt: DNAMAP-1727 (*Baltic Sea*)	1985–present	X	X	X	X	X	-	X	-
8	dk-30104	Hevring Bugt: DNAMAP-190004 (*Baltic Sea*)	1985–present	X	X	X	X	X	-	X	-

No.	IGMETS-ID	Site or programme name	Year-span	T	S	Oxy	Ntr	Chl	Mic	Phy	Zoo
9	dk-30108	Logstor Bredning: DNAMAP-3708-1 (*Baltic Sea*)	1980–present	X	X	X	X	X	-	X	-
10	dk-30109	Skive Fjord: DNAMAP-3727-1 (*Baltic Sea*)	1980–present	X	X	X	X	X	-	X	-
11	dk-30111	Alborg Bugt: DNAMAP-409 (*Baltic Sea*)	1981–present	X	X	X	X	X	-	X	-
12	dk-30112	Anholt East: DNAMAP-413 (*Baltic Sea*)	1981–present	X	X	X	X	X	-	X	-
13	dk-30113	Vejle Fjord: DNAMAP-4273 (*Baltic Sea*)	1982–present	X	X	X	X	X	-	X	-
14	dk-30114	Ven: DNAMAP-431 (*Baltic Sea*)	1979–present	X	X	X	X	X	-	X	-
15	dk-30115	Arkona: DNAMAP-444 (*Baltic Sea*)	1979–present	X	X	X	X	X	-	X	-
16	dk-30116	Mariager Fjord: DNAMAP-5503 (*Baltic Sea*)	1979–present	X	X	X	X	X	-	X	-
17	dk-30117	Horsens Fjord: DNAMAP-5790 (*Baltic Sea*)	1981–present	X	X	X	X	X	-	X	-
18	dk-30118	Roskilde Fjord: DNAMAP-60 (*Baltic Sea*)	1979–present	X	X	X	X	X	-	X	-
19	dk-30119	Lillebaelt-South: DNAMAP-6300043 (*Baltic Sea*)	1979–present	X	X	X	X	X	-	X	-
20	dk-30120	Lillebaelt-North: DNAMAP-6870 (*Baltic Sea*)	1979–present	X	X	X	X	X	-	X	-
21	dk-30121	Odense Fjord: DNAMAP-6900017 (*Baltic Sea*)	1979–present	X	X	X	X	X	-	X	-
22	dk-30122	Gniben: DNAMAP-925 (*Baltic Sea*)	1979–present	X	X	X	X	X	-	X	-
23	dk-30123	Storebaelt: DNAMAP-939 (*Baltic Sea*)	1982–present	X	X	X	X	X	-	X	-
24	dk-30124	Bornholm Deep: DNAMAP-bmpk2 (*Baltic Sea*)	1980–present	X	X	X	X	X	-	X	-
27	ee-10101	Pärnu Bay (*Gulf of Riga*)	1957–present	X	X	-	-	X	-	-	X
28	ee-10201	Tallinn Bay (*Gulf of Finland*)	1959–present	X	X	-	-	X	-	-	X
29	fi-30101	Bothnian Bay Region: Bo3+F2 (*Northern Baltic Sea*)	1959–present	X	X	X	X	X	X	X	X
30	fi-30102	Bothnian Sea Region: SR5+US5b+F64 (*Northern Baltic Sea*)	1959–present	X	X	X	X	X	X	X	X

No.	IGMETS-ID	Site or programme name	Year-span	T	S	Oxy	Ntr	Chl	Mic	Phy	Zoo
31	fi-30103	Gulf of Finland Region: LL3A+LL7+LL12 (*Northern Baltic Sea*)	1959–present	X	X	X	X	X	X	X	X
32	fi-30104	Northern Baltic Proper Region: BY15+BY38+LL17+LL23 (*Northern Baltic Sea*)	1959–present	X	X	X	X	X	X	X	X
33	lv-10101	Station 121 (*Gulf of Riga*)	1959–present	X	X	-	-	X	-	-	X
34	lv-10201	Eastern Gotland Basin (*Central Baltic Sea*)	1959–present	X	X	X	X	X	-	-	X
35	pl-30101	Gdansk Basin (*Baltic Sea*)	1959–present	X	X	-	X	X	X	X	X
36	pl-30102	Bornholm Basin (*Baltic Sea*)	1959–present	X	X	-	X	X	X	X	X
37	pl-30103	Pomeranian Bay (*Baltic Sea*)	1979–present	X	X	-	X	X	X	X	-
38	pl-30104	Southern Gotland Basin (*Baltic Sea*)	1959–present	X	X	X	-	X	-	-	X
39	se-50101	SMHI A17 (*Sweden*)	1982–present	X	X	X	X	X	X	X	X
40	se-50102	SMHI Anholt East (*Kattegat*)	1959–present	X	X	X	X	X	X	X	X
41	se-50103	SMHI Slaggo (*Sweden*)	1959–present	X	X	X	X	X	X	X	X

Mediterranean Sea

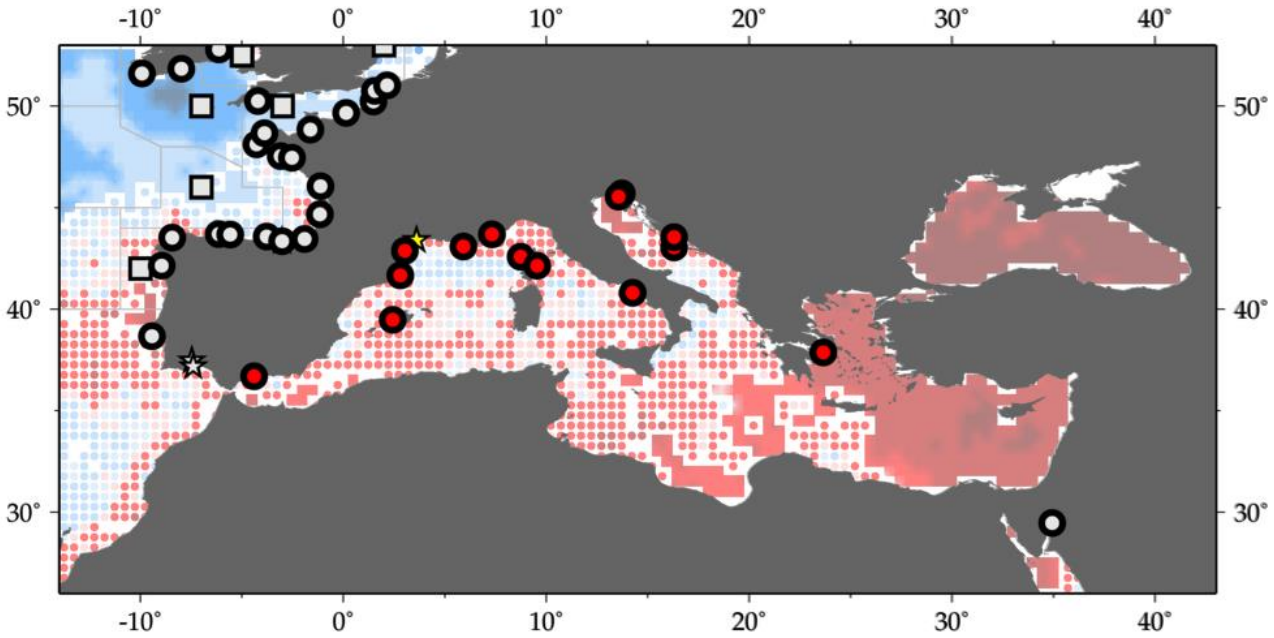

Figure 4.9. Map of IGMETS-participating Mediterranean Sea time series on a background of a 10-year time-window (2003–2012) sea surface temperature trends. At the time of this report, the Mediterranean Sea consisted of 16 time series (coloured symbols of any type; see also Table 4.5), of which one was from estuarine areas (yellow stars). Uncoloured (gray) symbols indicate time series being addressed in a different subregion (e.g. North Atlantic Proper, Figure 4.1/Table 4.3).

Table 4.5. Regional listing of participating time series for the IGMETS Mediterranean Sea. Participating countries: Belgium (be), Spain (es), France (fr), Greece (gr), Croatia (hr), Italy (it), Slovenia (si).

No.	IGMETS-ID	Site or programme name	Year-span	T	S	Oxy	Ntr	Chl	Mic	Phy	Zoo
1	be-10101	PHYTOCLY Time Series *(Bay of Calvi)*	1988–present	-	-	-	X	X	-	-	-
2	es-30301	Blanes Bay *(Northwest Mediterranean)*	1992–present	X	X	-	X	X	X	-	-
3	es-50201	IEO Mallorca Baleares Station *(Mallorca Channel)*	1994–present	X	X	-	-	X	-	-	X
4	es-50301	IEO ECOMÁLAGA *(Alboran Sea)*	1992–present	X	X	-	X	X	-	-	X
5	fr-10101	Villefranche Point B *(Cote d'Azur)*	1995–present	-	-	-	-	-	-	-	X
6	fr-10201	Thau Lagoon *(Mediterranean Sea)*	1965–present	X	X	-	X	X	X	X	-
7	fr-50111	REPHY Diana Centre *(Mediterranean Sea)*	1987–present	X	X	X	X	X	-	X	-
8	fr-50112	REPHY Lazaret A *(Western Mediterranean)*	1987–present	X	X	X	-	X	-	X	-

No.	IGMETS-ID	Site or programme name	Year-span	T	S	Oxy	Ntr	Chl	Mic	Phy	Zoo
9	fr-50113	REPHY Parc Leucate 2 *(Mediterranean Sea)*	1987–present	X	X	-	-	X	-	X	-
10	fr-50114	REPHY Villefranche *(Mediterranean Sea)*	1995–present	X	X	-	-	-	-	X	-
11	gr-10101	Saronikos Gulf S11 *(Aegean Sea)*	1987–present	-	-	-	-	X	-	-	X
12	hr-10101	Stoncica *(Central Adriatic Sea)*	1959–present	-	-	-	-	-	X	-	X
13	hr-10102	Kastela Bay *(Central Adriatic Sea)*	1994–present	-	-	-	-	-	X	-	-
14	it-30101	Gulf of Naples LTER-MC *(Tyrrhenian Sea)*	1984–present	X	X	-	X	X	-	X	X
15	it-30201	C1-LTER Gulf of Trieste *(Northern Adriatic Sea)*	1970–present	-	-	-	-	-	-	-	X
16	si-10101	Gulf of Trieste – MBS Buoy *(Northern Adriatic Sea)*	1990–present	X	X	X	X	X	-	X	-

4.6 References

Beaugrand, G., Conversi, A., Chiba, S., Edwards, M., Fonda-Umani, S., Greene, C., Mantua, N., *et al*. 2015. Synchronous marine pelagic regime shifts in the Northern Hemisphere. Philosophical Transactions of the Royal Society B, 370: (20130272), doi:10.1098/rstb.2013.0272.

Behrenfeld, M. J., O'Malley, R. T., Boss, E. S., Westberry, T. K., Graff, J. R., Halsey, K. H., Milligan, A. J., *et al*. 2015. Revaluating ocean warming impacts on global phytoplankton. Nature Climate Change, 5: doi:10.1038/NCLIMATE2838.

Benazzouz, A., Demarcq, H., and González-Nuevo, G. 2015. Recent changes and trends of the upwelling intensity in the Canary Current Large Marine Ecosystem. *In* Oceanographic and biological features in the Canary Current Large Marine Ecosystem, pp. 321–330. Ed. by L. Valdés, and I. Déniz-González. IOC-UNESCO, IOC Technical Series, No. 115. 383 pp.

Bode, A., Estévez, M. G., Varela, M., and Vilar, J. A. 2015. Annual trend patterns of phytoplankton species abundance belie homogeneous taxonomical group responses to climate in the NE Atlantic upwelling. Marine Environmental Research, 110: 81–91.

Bode, A., Hare, J., Li, W. K. W., Morán, X. A. G., and Valdés, L. 2011. Chlorophyll and primary production in the North Atlantic. *In* ICES status report on climate change in the North Atlantic, pp. 77–102. Ed. by P. C. Reid, and L. Valdés. ICES Cooperative Research Report No. 310. 262 pp.

Boyce, D. G., Dowd, M., Lewis, M. R., and Worm, B. 2014. Estimating global chlorophyll changes over the past century. Progress in Oceanography, 122: 163–173.

Carstensen, J., Andersen, J. H., Gustafsson, B. G., and Conley, D. J. 2014. Deoxygenation of the Baltic Sea during the last century. Proceedings of the National Academy of Sciences of the United States of America, 111(15): 5628–5633.

Demarcq, H., and Bénazzouz, A. 2015. Trends in phytoplankton and primary productivity off Northwest Africa. *In* Oceanographic and biological features in the Canary Current Large Marine Ecosystem, pp. 331–342. Ed. by L. Valdés, and I. Déniz-González. IOC-UNESCO, IOC Technical Series, No. 115. 383 pp.

Dickson, R. R., and Brown, J. 1994. The production of North Atlantic Deep Water: Sources, rates, and pathways. Journal of Geophysical Research, C. Oceans, 99(C6): 12319–12341.

Feistel, R., Nausch, G., and Wasmund, N. E. 2008. State and evolution of the Baltic Sea, 1952-2005. Wiley Interscience, Hoboken, NJ, USA. 703 pp.

Fisher, J. A. D., Casini, M., Frank, K. T., Möllmann, C., Leggett, W. C., and Daskalov, G. 2015. The importance of within-system spatial variation in drivers of marine ecosystem regime shifts. Philosophical Transactions of the Royal Society B, 370: (20130271), doi:10.1098/rstb.2013.0271.

Goffart, A., Hecq, J-H., and Legendre, L. 2015. Drivers of the winter-spring phytoplankton bloom in a pristine NW Mediterranean site, the Bay of Calvi (Corsica): A long-term study (1979-2011). Progress in Oceanography, 137: 121–139.

Hátún, H., Payne, M. R., Beaugrand, G., Reid, P. C., Sando, A. B., Drange, H., Hansen, B., *et al*. 2009. Large bio-geographical shifts in the north-eastern Atlantic Ocean: From the subpolar gyre, via plankton, to blue whiting and pilot whales. Progress in Oceanography, 80: 149–162.

Heath, M. R., and Beare, D. J. 2008. New primary production in northwest European shelf seas, 1960-2003. Marine Ecology Progress Series, 363: 183–203.

HELCOM. 2009. Eutrophication in the Baltic Sea - An integrated thematic assessment of the effects of nutrient enrichment and eutrophication in the Baltic Sea region. Baltic Sea Environment Proceedings, 115B. 148 pp.

HELCOM. 2014. Eutrophication status of the Baltic Sea 2007-2011. Baltic Sea Environment Proceedings, 143. 40 pp.

Hemery, G., D'Amico, F., Castege, I., Dupont, B., D'Elbee, J., Lalanne, Y., and Mouches, C. 2008. Detecting the impact of oceano-climatic changes on marine ecosystems using a multivariate index: The case of the Bay of Biscay (North Atlantic-European Ocean). Global Change Biology, 14: 27–38.

Hernández-Fariñas, T., Soudant, D., Barillé, L., Belin, C., Lefebvre, A., and Bacher, C. 2014. Temporal changes in the phytoplankton community along the French coast of the eastern English Channel and the southern Bight of the North Sea. ICES Journal of Marine Science, 71: 821–833.

Hinder, S. L., Hays, G. C., Edwards, M., Roberts, E., Walne, A. W., and Gravenor, M. B. 2012. Changes in marine dinoflagellate and diatom abundance under climate change. Nature Climate Change, 2: 271–275.

Hoegh-Guldberg, O., Cai, R., Poloczanska, E. S., Brewer, P. G., Sundby, S., Hilmi, K., Fabry, V. J., *et al.* 2014. The Ocean. *In* Climate Change 2014: Impacts, Adaptation, and Vulnerability. Part B: Regional Aspects, pp. 1655–1731. Ed. by V. R. Barros, C. B. Field, D. J. Dokken, M. D. Mastrandrea, K. J. Mach, T. E. Bilir, M. Chatterjee, *et al.* Contribution of Working Group II to the Fifth Assessment Report of the Intergovernmental Panel on Climate Change, Cambridge University Press, Cambridge and New York. 688 pp.

Hurrell, J. W., and Dickson, R. R. 2004. Climate variability over the North Atlantic. *In* Marine Ecosystems and Climate Variation - The North Atlantic, pp. 15–31. Ed. by N. C. Stenseth, G. Ottersen, J. W. Hurrell, and A. Belgrano. Oxford University Press, Oxford. 252 pp.

Hurrell, J., Meehl, G. A., Bader, D., Delworth, T. L., Kirtman, B., and Wielicki, B. 2009. A unified modeling approach to climate system prediction. Bulletin of the American Meteorological Society, 90(12): 1819–1832.

Knudsen, M. F., Seidenkrantz, M-S., Jacobsen, B. H., and Kuijpers, A. 2011. Tracking the Atlantic Multidecadal Oscillation through the last 8,000 years. Nature Communications, 2(178): doi:10.1038/ncomms1186.

Lennartz, S. T., Lehmann, A., Herrford, J., Malien, F., Hansen, H-P., Biester, H., and Bange, H. W. 2014. Long-term trends at the Time Series Station Boknis Eck (Baltic Sea), 1957-2013: does climate change counteract the decline in eutrophication? Biogeosciences, 11: 6323–6339.

Leterme, S. C., Seuront, L., and Edwards, M. 2006. Differential contribution of diatoms and dinoflagellates to phytoplankton biomass in the NE Atlantic Ocean and the North Sea. Marine Ecology Progress Series, 312: 57–65.

Levitus, S., Antonov, J. I., Boyer, T. P., and Stephens, C. 2000. Warming of the world ocean. Science, 287: 2225–2229.

Longhurst, A. 2007. Ecological Geography of the Sea, 2nd edn. Academic Press. 560 pp.

Llope, M., Anadón, R., Sostres, J. A., and Viesca, L. 2007. Nutrients dynamics in the southern Bay of Biscay (1993-2003): Winter supply, stoichiometry, long-term trends, and their effects on the phytoplankton community. Journal of Geophysical Research, 112: doi:10.1029/2006JC003573.

Marshall, J., Kushnir, Y., Battisti, D., Chang, P., Czaja, A., Dickson, R., Hurrell, J., *et al.* 2001. North Atlantic climate variability: phenomena, impacts and mechanisms. International Journal of Climatology, 21: 1863–1898.

McGinty, N., Power, A. M., and Johnson, M. P. 2012. Trophodynamics and stability of regional scale ecosystems in the Northeast Atlantic. ICES Journal of Marine Science, 69: 764–775.

McGregor, H. V., Dima, M., Fischer, H. W., and Mulitza, S. 2007. Rapid 20th-century increase in coastal upwelling off Northwest Africa. Science, 315: 637–639.

McQuatters-Gollop, A., Raitsos, D. E., Edwards, M., Pradhan, Y., Mee, L. D., Lavender, S. J., and Attrill, M. J. 2007. A long-term chlorophyll dataset reveals regime shift in North Sea phytoplankton biomass unconnected to increasing nutrient levels. Limnology and Oceanography, 52: 635–648.

Meyer-Gutbrod, E. L., Greene, C. H., Sullivan, P. J., and Pershing, A. J. 2015. Climate-associated changes in prey availability drive reproductive dynamics of the North Atlantic right whale population. Marine Ecology Progress Series, 535: 243–258.

O'Brien, T. D., Li, W. K. W., and Morán, X. A. G. (Eds). 2012. ICES Phytoplankton and Microbial Plankton Status Report 2009/2010. ICES Cooperative Research Report No. 313. 196 pp.

Pardo, P. C., Padín, X. A., Gilcoto, M., Farina-Busto, L., and Pérez, F. F. 2011. Evolution of upwelling systems coupled to the long-term variability in sea surface temperature and Ekman transport. Climate Research, 48: 231–246.

Pérez, F. F., Padin, X. A., Pazos, Y., Gilcoto, M., Cabanas, M., Pardo, P. C., Doval, M. D., *et al*. 2010. Plankton response to weakening of the Iberian coastal upwelling. Global Change Biology, 16: 1258–1267.

Plourde, S., Grégoire, F., Lehoux, C., Galbraith, P. S., and Castonguay, M. 2014. Effect of environmental variability on the Atlantic Mackerel (*Scomber scombrus* L.) stock dynamics in the Gulf of St. Lawrence. DFO Canadian Science Advisory Secretariat Research Document, 2014/092. 30 pp.

Reid, P. C., Edwards, M., McQuatters-Gollop, A., Beaugrand, G., Bresnan, E., Brierley, A., Davidson, K., *et al.* 2010. Charting Progress 2 Healthy and Biological Diverse Seas Feeder Report: Section 3.3: Plankton. *In* Charting Progress 2 Healthy and Biological Diverse Seas Feeder Report, pp. 286–377. Ed. by M. Frost, and J. Hawkridge. Department for Environment Food and Rural Affairs on behalf of UKMMAS, London.

Richardson, A. J., and Schoeman, D. S. 2004. Climate impact on plankton ecosystems in the Northeast Atlantic. Science, 305: 1609–1612.

Santos, F., Gómez-Gesteira, M., deCastro, M., and Álvarez, I. 2012. Variability of coastal and ocean water temperature in the upper 700 m along the Western Iberian Peninsula from 1975 to 2006. PLoS ONE, 7(12): e50666), doi:10.1371/journal.pone.0050666.

Suikkanen, S., Pulina, S., Engström-Öst, J., Lehtiniemi, M., Lehtinen, S., and Brutemark, A. 2013. Climate change and eutrophication induced shifts in northern summer plankton communities. PLoS ONE, 8(6): e66475, doi:10.1371/journal.pone.0066475.

Tremblay, J. E., and Gagnon, J. 2009. The effects of irrandiance and nutrient supply on the productivity of Arctic waters: a perspective on climate change. *In* Influence of Climate Change on the Changing Arctic and Sub-Arctic Conditions, pp. 73–93. Ed. by J. C. J. Nihoul, and A. G. Kostianov. Springer, Netherlands. 232 pp.

Worthington, L. V. 1986. On the North Atlantic circulation. Johns Hopkins Oceanographic Studies, 6: 1–110.

Zhai, L., Platt, T., Tang, C., Sathyendranath, S., and Walne, A. 2013. The response of phytoplankton to climate variability associated with the North Atlantic Oscillation. Deep-Sea Research II, 93: 159–168.